A&A 453, 809–815 (2006)
DOI: 10.1051/0004-6361:20053632

Astronomy & Astrophysics

The VIMOS-VLT Deep Survey⋆

Galaxy luminosity function per morphological type up to $z = 1.2$

O. Ilbert[1,7], S. Lauger[1], L. Tresse[1], V. Buat[1], S. Arnouts[1], O. Le Fèvre[1], D. Burgarella[1], E. Zucca[2], S. Bardelli[2], G. Zamorani[2], D. Bottini[3], B. Garilli[3], V. Le Brun[1], D. Maccagni[3], J.-P. Picat[4], R. Scaramella[5], M. Scodeggio[3], G. Vettolani[5], A. Zanichelli[5], C. Adami[1], M. Arnaboldi[6], M. Bolzonella[7], A. Cappi[2], S. Charlot[8,9], T. Contini[4], S. Foucaud[3], P. Franzetti[3], I. Gavignaud[4,12], L. Guzzo[10], A. Iovino[10], H. J. McCracken[9,11], B. Marano[7], C. Marinoni[1], G. Mathez[4], A. Mazure[1], B. Meneux[1], R. Merighi[2], S. Paltani[1], R. Pello[4], A. Pollo[10], L. Pozzetti[2], M. Radovich[6], M. Bondi[5], A. Bongiorno[7], G. Busarello[6], P. Ciliegi[2], Y. Mellier[9,11], P. Merluzzi[6], V. Ripepi[6], and D. Rizzo[4]

[1] Laboratoire d'Astrophysique de Marseille (UMR 6110), CNRS-Université de Provence, BP 8, 13376 Marseille Cedex 12, France
e-mail: olivier.ilbert1@bo.astro.it
[2] INAF - Osservatorio Astronomico di Bologna, via Ranzani 1, 40127 Bologna, Italy
[3] INAF - IASF, via Bassini 15, 20133 Milano, Italy
[4] Laboratoire d'Astrophysique de l'Observatoire Midi-Pyrénées (UMR 5572), CNRS-Université Paul Sabatier, 14 avenue E. Belin, 31400 Toulouse, France
[5] INAF - IRA, via Gobetti 101, 40129 Bologna, Italy
[6] INAF - Osservatorio Astronomico di Capodimonte, via Moiariello 16, 80131 Napoli, Italy
[7] Università di Bologna, Dipartimento di Astronomia, via Ranzani 1, 40127 Bologna, Italy
[8] Max-Planck-Institut für Astrophysik, Karl-Schwarzschild-Str. 1, 85740 Garching bei München, Germany
[9] Institut d'Astrophysique de Paris (UMR 7095), 98 bis boulevard Arago, 75014 Paris, France
[10] INAF - Osservatorio Astronomico di Brera, via Brera 28, 20121 Milano, Italy
[11] Observatoire de Paris-LERMA, 61 avenue de l'Observatoire, 75014 Paris, France
[12] European Southern Observatory, Karl-Schwarzschild-Str. 2, 85748 Garching bei München, Germany

Received 14 June 2005 / Accepted 16 January 2006

ABSTRACT

Aims. We have computed the evolution of the rest-frame B-band luminosity function (LF) for bulge and disk-dominated galaxies since $z = 1.2$.
Methods. We use a sample of 605 spectroscopic redshifts with $I_{AB} \leq 24$ in the Chandra Deep Field South from the VIMOS-VLT Deep Survey, 3555 galaxies with photometric redshifts from the COMBO-17 multi-color data, coupled with multi-color HST/ACS images from the Great Observatories Origin Deep Survey. We split the sample in bulge- and disk-dominated populations on the basis of asymmetry and concentration parameters measured in the rest-frame B-band.
Results. We find that at $z = 0.4$–0.8, the LF slope is significantly steeper for the disk-dominated population ($\alpha = -1.19 \pm 0.07$) compared to the bulge-dominated population ($\alpha = -0.53 \pm 0.13$). The LF of the bulge-dominated population is composed of two distinct populations separated in rest-frame color: 68% of red $(B-I)_{AB} > 0.9$ and bright galaxies showing a strongly decreasing LF slope $\alpha = +0.55 \pm 0.21$, and 32% of blue $(B-I)_{AB} < 0.9$ and more compact galaxies which populate the LF faint-end. We observe that red bulge-dominated galaxies are already well in place at $z \simeq 1$, but the volume density of this population is increasing by a factor 2.7 between $z \sim 1$ and $z \sim 0.6$. It may be related to the building-up of massive elliptical galaxies in the hierarchical scenario. In addition, we observe that the blue bulge-dominated population is dimming by 0.7 mag between $z \sim 1$ and $z \sim 0.6$. Galaxies in this faint and more compact population could possibly be the progenitors of the local dwarf spheroidal galaxies.

Key words. surveys – Galaxy: evolution – galaxies: luminosity function, mass function – galaxies: fundamental parameters

1. Introduction

A central issue to understand galaxy formation is to study the building up of the Hubble sequence. One approach is to measure the evolution in numbers and luminosity of different galaxy types using the luminosity function (LF). To this effect, large samples of galaxies are required with a robust estimate of distances, luminosities and morphological types.

At low as well as at high redshifts, most luminosity functions have been measured using galaxy samples classified by spectral type (e.g. Madgwick et al. 2002; de Lapparent et al. 2003) or by photometric type (e.g. Lilly et al. 1995; Wolf et al. 2003; Zucca et al. 2006). The direct interpretation of these results in the framework of a galaxy formation scenario is not straightforward since galaxies move from one spectral class to another by a passive evolution of their stellar population. Another way to define the galaxy type is to define a morphological type from the measurement of the structural parameters of the galaxies from image analysis. Even if star formation evolution could affect galaxy

⋆ Based on data obtained with the European Southern Observatory on Paranal, Chile.

morphologies, a morphological classification is less sensitive to the star formation history than a classification based on the spectral energy distribution. This classification is also more robust to follow similar galaxies at different redshifts.

Unfortunately, it is difficult to assemble large samples of morphologically classified galaxies with measured spectroscopic redshifts for $z > 0.3$, as high resolution images are required to perform a morphological classification and a large amount of telescope time is needed to measure spectroscopic redshifts. This is why the largest samples of galaxies with both high resolution morphology and spectroscopic redshifts are not exceeding ∼300−400 spectroscopic redshifts (e.g. Brinchmann et al. 1998; Cassata et al. 2005). Larger samples of galaxies are obtained using the photometric redshifts method (e.g. Wolf et al. 2005; Bell et al. 2005), but a major drawback of the photometric redshift method is the difficulty to control the systematic uncertainties which are affecting the redshift estimate and to quantify the impact of these systematics on the LF estimate.

This paper presents a study of the evolution of the galaxy LF as a function of morphological type. We use the spectroscopic redshifts from the VIMOS VLT Deep Survey on the Chandra Deep Field South (CDFS; Le Fèvre et al. 2004). The spectroscopic sample selected at $I_{\rm AB} \leq 24$ is twice larger than previous spectroscopic samples at similar redshifts. We consolidate the results using 3555 photometric redshifts estimated from the COMBO-17 multi-color data. We check that photometric redshifts are not creating a systematic bias in the LF measurement from a detailed comparison between photometric redshift and spectroscopic redshift results. The morphological classification is performed using the multi-color images of the Hubble Space Telescope-Advanced Camera for Surveys released by the Great Observatories Origin Deep Survey (Giavalisco et al. 2004). Different methods to perform the morphological classification of this sample are presented in the companion paper Lauger et al. (2006) and compared with a visual classification of the sample. A single wavelength rest-frame morphological classification can be applied over the whole redshift range. Lauger et al. (2006) show that this classification can separate two robust classes: bulge- and disk-dominated galaxies. This paper presents the measurement of the LF evolution per morphological type, based on this single wavelength rest-frame morphological classification.

We use a flat lambda ($\Omega_{\rm m} = 0.3$, $\Omega_\Lambda = 0.7$) cosmology with $h = H_0/100$ km s^{-1} Mpc^{-1}. Magnitudes are given in the AB system.

2. Data set description

We use the high-resolution images provided by the Great Observatories Origin Deep Survey (GOODS, Giavalisco et al. 2004) on the Chandra Deep Field South (CDFS) to perform the study of the galaxy morphology. The images have been acquired with the Hubble Space Telescope-Advanced Camera for Surveys (HST/ACS). The field covers 160 arcmin^2 and has been observed in four bands $F435W$, $F606W$, $F775W$, $F850LP$ (noted hereafter B, V, i, z respectively).

We use the spectroscopic redshifts from the VIMOS VLT Deep Survey (VVDS) on the CDFS (Le Fèvre et al. 2004). The spectroscopic observations have been conducted with the multi-object spectrograph VIMOS on the VLT-ESO Melipal. The spectroscopic targets are selected on a pure magnitude criterion $17.5 \leq I_{\rm AB} \leq 24$ from the ESO Imaging Survey (Arnouts et al. 2001). The sample used in this paper is limited to the area covered by GOODS. Our sample contains 670 objects (605 galaxies, 60 stars, 5 QSOs) with a secure measurement of the redshift (confidence level greater than 80%) and a mean redshift of 0.76.

Multi-color data from COMBO-17 are available on the CDFS field (Wolf et al. 2004). These data consist in 12 medium-band filters and 5 broad-band filters from 3500 Å to 9300 Å. We also use the near-infrared J and K band data (21 600 Å) from the ESO Imaging Survey (Arnouts et al. 2001).

3. Photometric redshifts with *Le Phare*

We apply the code *Le Phare*[1] (S. Arnouts & O. Ilbert) on the COMBO-17 multi-color data completed by the NIR data from EIS to compute photometric redshifts for the complete CDFS sample. The photometric redshifts are measured with a standard χ^2 from the best fit template on multi-color data (Arnouts et al. 2002). Our set of templates is composed of four observed spectra from Coleman et al. (1980) and one starburst SED from GISSEL (Bruzual & Charlot 2003). These 5 templates have been interpolated to increase the accuracy of the redshift estimate.

Our photometric redshift code significantly improves the standard χ^2 method (Ilbert et al. 2006). We compute the average difference in each band between the observed apparent magnitudes and the predicted apparent magnitudes derived from the best fit template for a restricted sample of 67 bright galaxies ($I_{\rm AB} < 20$) with a spectroscopic redshift. These differences never exceed 0.2 and have an average value over all filters of 0.06 mag. We correct the predicted apparent magnitudes from these systematic differences. This method of calibration corrects for the small uncertainties existing in the filter transmission curves or in the calibration of the photometric zero-points.

The comparison between photometric redshifts and spectroscopic redshifts is shown in Fig. 1. We only use the most secure spectroscopic redshifts with a confidence level greater than 95% (Le Fèvre et al. 2005). The fraction of catastrophic errors ($\Delta z/(1+z) > 0.1$) in photometric redshifts estimates is 1.1% and the accuracy of the measurement is $\sigma_{\Delta z/(1+z)} = 0.046$. 295 stars are removed from the sample which satisfy simultaneously a morphological criterion (SExtractor CLASS_STAR parameter greater than 0.975) and a χ^2 criterion (χ^2(gal) − χ^2(star) > 0). Up to $z = 1.2$ and for $I_{\rm AB} \leq 24$, the sample contains 3555 photometric redshifts of galaxies associated with ACS/HST images.

4. Morphological classification

We measure asymmetry (A) and concentration (C) parameters on the ACS/HST images (Abraham et al. 1996; Conselice et al. 2000; Lauger et al. 2005; Menanteau et al. 2006). The concentration of light is defined as the ratio between the radii which contain 80% and 20% of the total flux of the galaxy, respectively. The asymmetry is obtained by computing the difference pixel per pixel of the original image and of its 180° rotation. We adopt these parameters to define our morphological classes since this classification is automatic, quantitative and reproducible.

Importantly, and thanks to the multi-color coverage of the ACS/HST images, we can measure the parameters A and C in the same rest-frame B-band from $z = 0$ up to $z \sim 1.2$ (Cassata et al. 2005). In this way, we reduce the effect of a morphological k-correction which gives a more patchy appearance to the galaxies at higher redshift when observations are restricted to one band (e.g. Kuchinski et al. 2000; Burgarella et al. 2001).

[1] www.lam.oamp.fr/arnouts/LE_PHARE.html

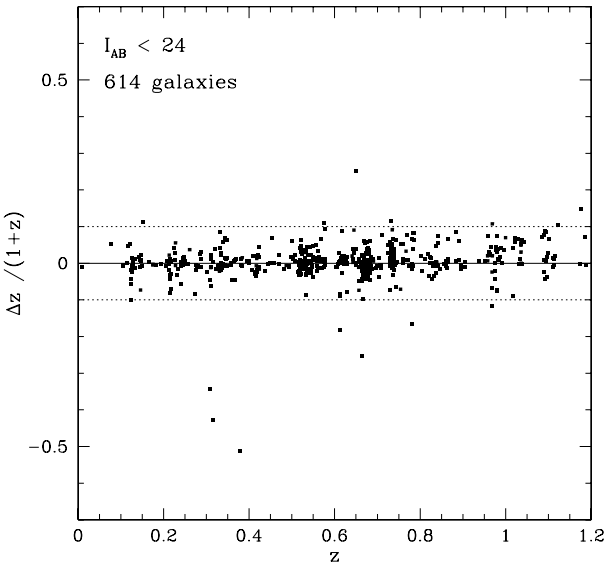

Fig. 1. Difference between VVDS spectroscopic redshifts and photometric redshifts (Δz) as a function of the spectroscopic redshift.

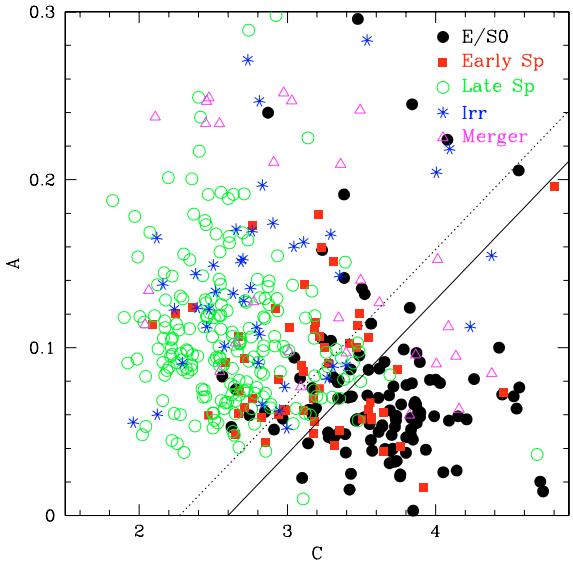

Fig. 2. Distribution in the A–C diagram of the eyeball classified galaxies with a spectroscopic redshift. The solid circles correspond to galaxies visually classified as elliptical-S0, the solid squares to early spirals, the open circles to late spirals, the star to irregulars and open triangles to mergers. The solid line is the empirical criterion $A = 0.0917C - 0.2383$ we have adopted to separate bulge- and disk-dominated populations. The dotted line corresponds to the criterion $A = 0.0917C - 0.2083$.

To relate the quantitative parameters $A - C$ to the Hubble sequence, we calibrate our morphological classes in the $A-C$ plane with a visual classification of galaxies. We adopt the empirical criterion $A = 0.0917C - 0.2383$ to separate the bulge-dominated population from the disk-dominated population (solid line of Fig. 2). This criterion is chosen to maximize the separation between E/S0 and spiral/irregular classified galaxies. We show in the companion paper Lauger et al. (2006) that the bulge-dominated population defined with $A \leq 0.0917C - 0.2383$ contains 8.9% of late spiral/irregular galaxies and that the disk-dominated population includes 8.3% of E/S0 galaxies down to $I_{\rm AB} \leq 24$. The bulge-dominated area contains also 21.2% of early spiral galaxies but the visual differentiation between faint early spiral galaxies and lenticular galaxies is strongly subjective.

5. Galaxy luminosity function with *ALF*

We derive the LF using the Algorithm for Luminosity Function (ALF) described in Ilbert et al. (2005). ALF includes 4 standard estimators of the LF which are the $1/V_{\rm max}$, C^+, SWML and STY. Combining these 4 estimators allows us to check the robustness of our estimate against spatial inhomogeneities, absolute magnitude binning, or spectral type incompleteness (Ilbert et al. 2004). We measure k-corrections from a procedure of template fitting on the multi-color data (Ilbert et al. 2005), using either the photometric redshift or the spectroscopic redshift according to the sample used.

We measure the LF in the rest-frame B Johnson band. At the average redshift $z \sim 0.76$ of this I-selected sample, this choice of the rest-frame B-band limits the model dependency of the absolute magnitudes (Ilbert et al. 2005), and minimizes any possible biases due to the mix of spectral types (Ilbert et al. 2004).

6. Results

The values given in this section are obtained using the photometric redshift sample to increase the accuracy of the measurements. However, we systematically check that the results obtained with spectroscopic redshifts and photometric redshifts are fully consistent.

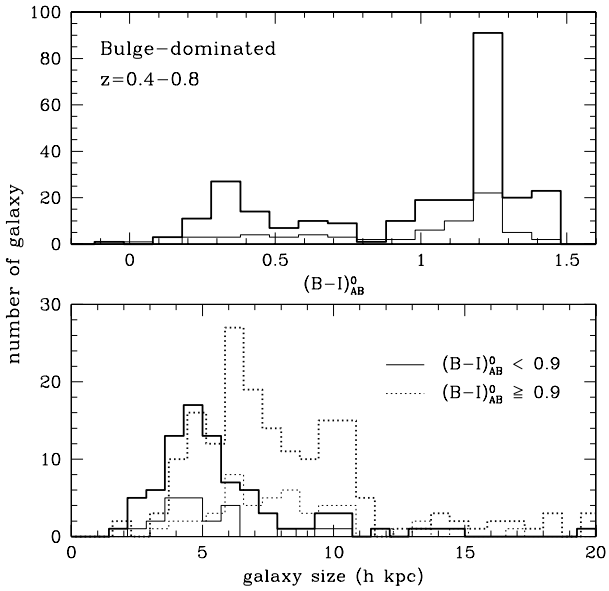

Fig. 3. *Top panel*: the distribution of the $(B-I)^0_{\rm AB}$ rest-frame colors for the bulge-dominated population. *Bottom panel*: galaxy size distribution for the red bulge-dominated population (dotted line) and for the blue bulge-dominated population (solid line). For both panels, the thick lines correspond to the photometric redshift sample and the thin lines to the spectroscopic redshift sample.

6.1. A blue bulge-dominated population

We observe a blue population of bulge-dominated galaxies as already observed by e.g. Im et al. (2001), Menanteau et al. (2004), Cross et al. (2004). For both the spectroscopic and photometric redshift samples, the $(B-I)^0_{\rm AB}$ rest-frame colors of the bulge-dominated population present a bimodal distribution (see upper panel of Fig. 3). We split the bulge-dominated population into two sub-samples separated in rest-frame color by $(B-I)^0_{\rm AB} = 0.9$

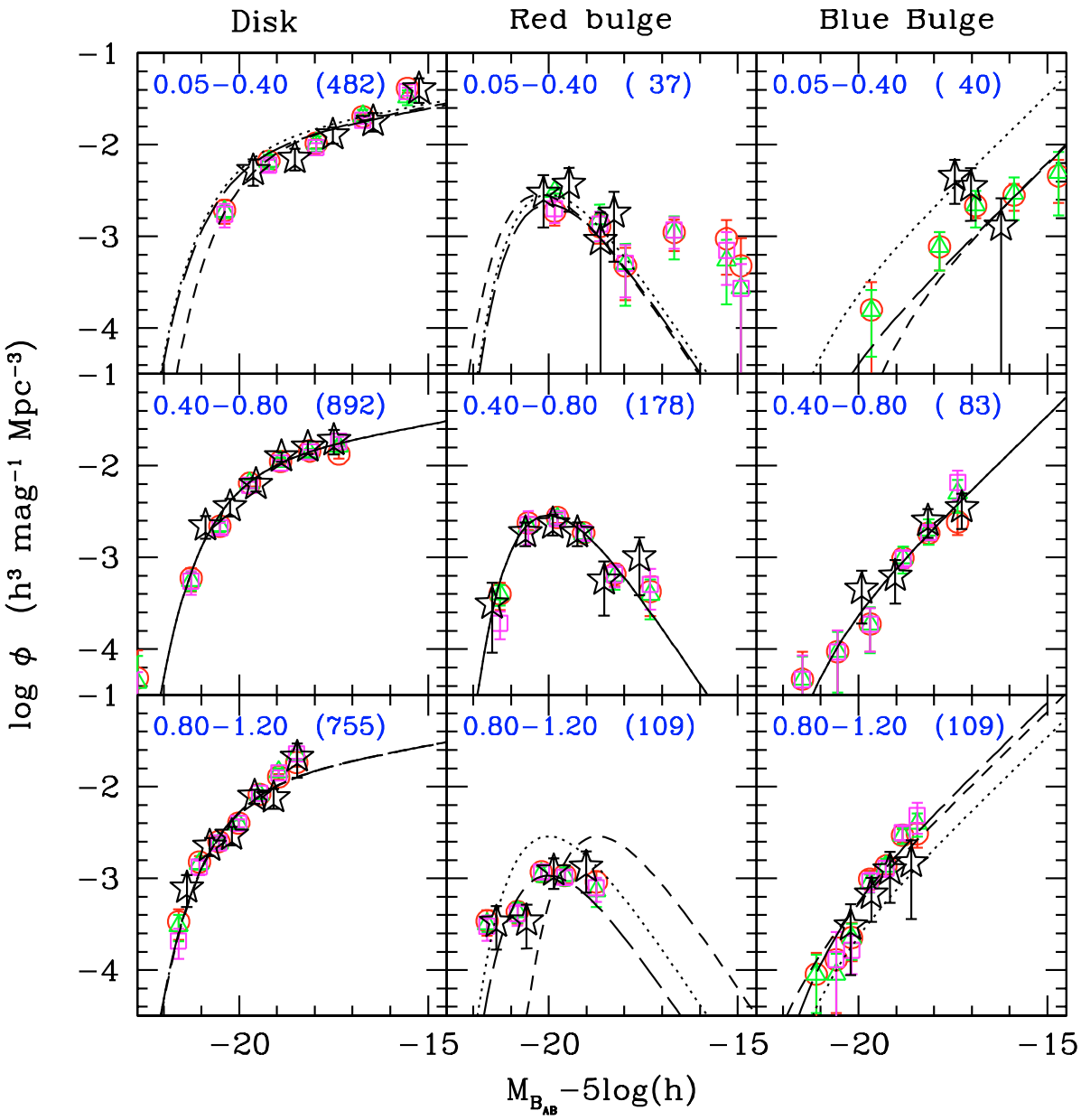

Fig. 4. Evolution of the Luminosity Function for galaxies classified in morphological types from $z = 0.05$ up to $z = 1.2$. Open stars correspond to the LFs measured with the spectroscopic redshift sample using the $1/V_{\rm max}$ estimator. All the other results are obtained using the photometric redshift sample. The left panels correspond to the LF of the disk-dominated population, the middle panels to the red bulge-dominated population and the right panels to the blue bulge-dominated population. The redshift bin and the corresponding number of galaxies is indicated in each panel. We adopt the following symbols for the various estimators: circles for the $1/V_{\rm max}$, triangles for the SWML, squares for the C^+ and solid lines for the STY (only at $z = 0.4$–0.8 where the LF shape is constrained). The STY fit derived in the redshift bin 0.4–0.8 is reported in each panel with dotted lines. The long dashed lines and short dashed lines correspond respectively to the fit obtained setting $\alpha - M^*$ (pure density evolution) and $\alpha - \Phi^*$ (pure luminosity evolution) at the values obtained at $z = 0.4$–0.8.

according to this bimodality. We measure 32%/68% of blue/red galaxies at $z = 0.4$–0.8, respectively. This fraction of blue bulge-dominated galaxies is similar to the proportion of 30% obtained by Cross et al. (2004) using a rest-frame color criterion $(U - V)_{\rm AB} > 1.7$ and a similar selection of $I_{\rm AB} \leq 24$.

To investigate farther the structural properties of this blue population, we use the Petrosian radius $r(\eta = 0.2)$ (see Lauger et al. 2005) and the angular distance to measure the physical size of the galaxy. Figure 3 (lower panel) shows the galaxy size distribution for blue and red bulge-dominated galaxies. The blue population, with an average size of 5.8 h kpc is more compact than the red population with an average size of 8.2 h kpc. The hypothesis that these two samples are extracted from the same population is rejected at 99.9% by a Kolmogorov-Smirnov test.

6.2. Shape of the LF versus morphology

We investigate the dependency of the LF shape on the morphological type. This analysis is performed in the redshift bin 0.4–0.8, a good compromise maximizing the number of galaxies and covering a large absolute magnitude range. The LFs of the disk- and bulge-dominated populations are shown in the middle panels of Fig. 4 and the corresponding Schechter parameters are given in Table 1. The LFs obtained with the

Table 1. Schechter parameters for the rest-frame B-band LF in the redshift bin 0.4−0.8 and the corresponding 1σ error. The parameters without associated errors are fixed. Values are given for the photometric redshift sample.

Type	Nb	α	$M^*_{\rm AB}(B) - 5\log(h)$ (mag)	ϕ^* ($\times 10^{-3}\ h^3\ {\rm Mpc}^{-3}$)
disk	892	$-1.19^{+0.07}_{-0.07}$	$-20.22^{+0.15}_{-0.15}$	$12.39^{+2.18}_{-2.01}$
bulge	261	$-0.53^{+0.13}_{-0.13}$	$-20.20^{+0.19}_{-0.20}$	$7.48^{+1.04}_{-1.11}$
red-bulge	178	$+0.55^{+0.21}_{-0.21}$	$-19.53^{+0.14}_{-0.15}$	$7.44^{+0.56}_{-0.56}$
blue-bulge	83	−2.00	$-20.95^{+0.63}_{-0.79}$	$0.16^{+0.16}_{-0.09}$

Table 2. Evolution of the Schechter parameters for the rest-frame B-band LF and associated 1σ errors. Values are given for the photometric redshift sample. The parameters without associated errors are set using the values measured at $z = 0.4$−0.8. At $z = 0.05$−0.4 and $z = 0.8$−1.2, we always provide the parameters for a pure luminosity and density evolution. When possible, we also provide the parameters for $M^* - \Phi^*$ let free to vary. When α is set, the STY errors on M^* and Φ^* are underestimated.

Type	z	Nb	α	$M^*_{\rm AB}(B) - 5\log(h)$ (mag)	ϕ^* ($\times 10^{-3}\ h^3\ {\rm Mpc}^{-3}$)
disk	0.05–0.40	482	−1.19	$-19.79^{+0.12}_{-0.11}$	12.39
	0.05–0.40	482	−1.19	−20.22	$10.95^{+0.58}_{-0.58}$
	0.05–0.40	482	−1.19	$-19.54^{+0.14}_{-0.15}$	$15.85^{+0.91}_{-0.87}$
	0.40–0.80	892	$-1.19^{+0.07}_{-0.07}$	$-20.22^{+0.15}_{-0.15}$	$12.39^{+2.18}_{-2.01}$
	0.80–1.20	755	−1.19	$-20.21^{+0.04}_{-0.04}$	12.39
	0.80–1.20	755	−1.19	−20.22	$12.44^{+0.51}_{-0.51}$
	0.80–1.20	755	−1.19	$-20.06^{+0.07}_{+0.07}$	$15.65^{+1.06}_{-0.98}$
red-bulge	0.05–0.40	37	+0.55	$-19.77^{+0.40}_{-0.39}$	7.44
	0.05–0.40	37	+0.55	−19.53	$5.79^{+1.23}_{-1.23}$
	0.40–0.80	178	$+0.55^{+0.21}_{-0.21}$	$-19.53^{+0.14}_{-0.15}$	$7.44^{+0.56}_{-0.56}$
	0.80–1.20	109	+0.55	$-18.23^{+0.09}_{-0.09}$	7.44
	0.80–1.20	109	+0.55	−19.53	$2.78^{+0.30}_{-0.30}$
	0.80–1.20	109	+0.55	$-19.76^{+0.09}_{-0.09}$	$3.05^{+0.29}_{-0.29}$
blue-bulge	0.05–0.40	40	−2.00	−20.95	$0.03^{+0.01}_{-0.01}$
	0.05–0.40	40	−2.00	$-19.11^{+0.22}_{-0.20}$	0.16
	0.40–0.80	83	−2.00	$-20.95^{+0.63}_{-0.79}$	$0.16^{+0.16}_{-0.09}$
	0.80–1.20	109	−2.00	−20.95	$0.38^{+0.04}_{-0.04}$
	0.80–1.20	109	−2.00	$-21.63^{+0.11}_{-0.10}$	0.16

photometric and the spectroscopic redshift samples are in very good agreement and no systematic trend in the shape is observed when using photometric redshifts.

The LF of the disk-dominated population presents a steep slope ($\alpha = -1.19 \pm 0.07$) which contrasts with the decreasing slope measured for the bulge-dominated population ($\alpha = -0.53 \pm 0.13$). This population of disk-dominated galaxies is the dominant population of galaxies at $z \sim 0.6$. From the integration of the LF up to $M_{B_{\rm AB}} - 5\log(h) = -17$, the disk-dominated population represents 74% of the whole galaxy population.

The slope measured for the bulge-dominated population ($\alpha = -0.53 \pm 0.13$, see Table 1) is steeper than previous LF measurement based on spectral type measurements (e.g. $\alpha = 0.52 \pm 0.20$ for Wolf et al. 2003, $\alpha = -0.27 \pm 0.10$ for Zucca et al. 2006). The presence of the faint blue bulge-dominated population explains this difference. The blue bulge-dominated population is composed of faint galaxies representing 67% of the bulge-dominated galaxies for $-19.5 < M_{B_{\rm AB}} - 5\log(h)$ but only 7.1% for $M_{B_{\rm AB}} - 5\log(h) < -19.5$. As the LF slope is extremely steep, the proportion of the observed blue galaxies is strongly dependent on the considered limit (here $M_{B_{\rm AB}} - 5\log(h) \leq -17$). On the contrary, the red bulge-dominated population is composed of bright galaxies and represents 92% of the bulge-dominated population for $M_{B_{\rm AB}} - 5\log(h) \leq -19.5$. The density of red bulge galaxies decreases toward fainter magnitudes with a strongly decreasing LF slope $\alpha = 0.55 \pm 21$. Between $-19.5 < M_{B_{\rm AB}} - 5\log(h) \leq -17$, the red bulge-dominated population represents only 5.7% of the whole population. The shape of the LF is in agreement with the measurement done by Cross et al. (2004) for red E/S0 galaxies ($\alpha = 0.35 \pm 0.59$, $M^*_{B_{\rm AB}} - 5\log(h) = -19.8 \pm 0.5$ mag at $0.5 < z < 0.75$). This selected sample of red bulge-dominated galaxies corresponds to the classical E/S0 population, composed of red and bright galaxies with a strongly decreasing LF slope. Blue and red bulge-dominated populations clearly exhibit different properties and need to be analysed separately.

6.3. Evolution of the LF

Figure 4 presents the evolution of the disk-, red bulge- and blue bulge-dominated populations from $z = 0.05$ up to $z = 1.2$. The Schechter parameters are given in Table 2. Since the LF slope is not constrained at $z > 0.8$, we set α to the value measured at $z = 0.4$−0.8.

The results obtained with the photometric redshift sample are fully in agreement with the results obtained with the spectroscopic redshift sample (see the open stars of Fig. 4). This comparison gives confidence that our measurement of the LF evolution is not due to systematic trends in photometric redshift estimates.

The LF of the disk-dominated galaxies evolves only mildly over the redshift range up to $z = 1.2$. The slope of the

disk-dominated galaxies in our sample is comparable to the local values obtained by Marinoni et al. (1999) ($\alpha = -1.10 \pm 0.07$ for S-Im eyeball classified galaxies) or by Nakamura et al. (2003) ($\alpha = -1.12 \pm 0.18$ for S-Im type defined with concentration parameter). No significant evolution of Φ^* is measured between $z = 0.05$ and $z = 1.2$ when testing for a pure density evolution (setting the $\alpha - M^*$ parameters, see Table 2). We measure only a small brightening of 0.4 mag when testing for pure luminosity evolution (setting the values of $\alpha - \Phi^*$). Leaving M^* and ϕ^* free (setting only the slope), we measure a brightening of $\Delta M* \sim 0.5$ mag with no significant evolution of Φ^* between $z = 0.05$ and $z = 1.2$.

The density of the red bulge-dominated population decreases at high redshift $z = 0.8-1.2$. We measure a decrease in density by a factor 2.7 between $z \sim 0.6$ and $z \sim 1$ for a pure density evolution (setting the $M^* - \alpha$ parameters). A pure luminosity evolution of the LF is not a good fit of the non-parametric data (see Fig. 4). Leaving M^* and ϕ^* free (setting only the slope), we measure a small brightening of 0.2 mag with a decrease of Φ^* by a factor 2 between $z \sim 0.6$ and $z \sim 1$, consistent with a pure density evolution. Due to the difficulty to sample the bright part of the red-bulge dominated LF at $z = 0.05-0.4$, no strong conclusions can be drawn in this low redshift range. The evolution of the LF for the red bulge-dominated population is opposite to the increase in density observed by Cross et al. (2004) between $z = 0.5-0.75$ and $z = 0.75-1$ but is in agreement with the result obtained by Ferreras et al. (2005) on the same field. Our results are fully consistent with the results from the VVDS based on spectroscopic redshifts and spectral type classification (Zucca et al. 2006). The observed evolution of the red bulge-dominated population in our analysis remains small in comparison to the strong decrease in density of the elliptical galaxies measured by Wolf et al. (2003) using spectral type classification and photometric redshifts. Our results instead show that the population of E/S0 galaxies is already mostly in place at $z \sim 1$.

The LF slope of the blue bulge-dominated population remains extremely steep in all the redshift bins. This population strongly evolves. To quantify the LF evolution of this population, we first set the $M^* - \alpha$ parameters to the $z = 0.4-0.8$ values and look for an evolution in Φ^*. We measure an increase in density of a factor 2.4 between $z = 0.4-0.8$ and $z = 0.8-1.2$. Using the same procedure, we set the $\alpha - \Phi^*$ parameters to the $z = 0.4-0.8$ values and look for an evolution in M^*. We measure a brightening of 0.7 mag between $z = 0.4-0.8$ and $z = 0.8-1.2$. The same trend is also present between $z = 0.05-0.4$ and $z = 0.4-0.8$. It is unlikely than a large fraction of this blue bulge-dominated population contains misclassified spiral galaxies at high redshifts as the visual inspection of the UV rest-frame images at $z \sim 1$ do not show star formation in the disc of these galaxies. If a large fraction of these blue bulge-dominated galaxies is including misclassified spiral galaxies at $z < 0.7$ as claimed by Ferreras et al. (2005), the observed evolution of the blue bulge-dominated galaxies should even be stronger than what we have reported here.

Since A and C are quantitative parameters and since the visual classification is strongly subjective, the separation between bulge- and disk-dominated galaxies in the $A - C$ plan is not a sharp limit. The area enclosed between $A \leq 0.0917C - 0.2383$ (solid line of Fig. 2) and $A \leq 0.0917C - 0.2083$ (dotted line of Fig. 2) contains a mix of different visual types. To quantify the impact of the adopted criterion on our conclusions, we recompute the LFs using the criteria $A \leq 0.0917C - 0.2083$ rather than $A \leq 0.0917C - 0.2383$. This less conservative criterion increases the contamination of blue late spiral galaxies in the bulge-dominated area. As expected, the LF normalization of the blue bulge-dominated galaxies increases by a factor 1.6–2. We have specifically used a conservative criterion throughout this paper ($A \leq 0.0917C - 0.2383$) to limit the fraction of late spiral/irregular galaxies in the bulge-dominated area. We have checked that only 12% of the blue-bulge dominated galaxies have been visually classified as late spiral or irregular galaxies. The LFs of the disk-dominated and of the red bulge-dominated galaxies remain unchanged and are little sensitive to the adopted criterion.

7. Discussion and conclusions

We derive the rest-frame B-band LF of galaxies classified in morphological types up to $z = 1.2$ in the CDFS using the VVDS spectroscopic sample of 605 galaxies, 3555 photometric redshifts from COMBO-17 multi-color data and the HST/ACS images from GOODS. We define bulge- and disk-dominated populations on the basis of $A-C$ parameters measured in the rest-frame B-band (Lauger et al. 2006). We show that the LF of the bulge-dominated population is the combination of two populations: a red and bright population making 68% of the bulge-dominated sample, and a blue population of more compact galaxies for the remaining 32% of the population. We observe a strong dependency of the LF shape on the morphological type. In the redshift range $0.4 < z < 0.8$, we measure a shallow slope $\alpha = +0.55 \pm 0.21$ for the red bulge-dominated population while the disk-dominated population shows a very steep slope $\alpha = -1.19 \pm 0.07$. The blue bulge-dominated population dominates the faint-end of the bulge-dominated LF. We emphasize that without morphological information, the blue bulge-dominated population can not be separated from the late spectral type population even if a composite fit of the LF (de Lapparent et al. 2003) is computed as an alternative when visual morphologies are not available.

We observe a small evolution of the disk-population. This is unexpected as the irregular galaxies included in our disk-dominated class are expected to evolve strongly (e.g. Brinchmann et al. 1998). As our one-wavelength $A-C$ parameters are not efficient to isolate the irregular or merger galaxies from the late spiral galaxies (see Fig. 2), this small evolution of the disk-dominated population could possibly be explained by cosmic variance in this small field, by the fact that spiral galaxies dominate the population of irregular galaxies, and by the fact that we are insensitive to the morphological k-correction effect.

We measure an increase in density of the red, bright (brighter than M^* at $z > 0.8$), bulge-dominated population with the age of the Universe. The observed evolution of the red bulge-dominated LF could be interpreted as evidence for the build-up of massive elliptical galaxies from merging and accretion of smaller galaxies in a hierarchical scenario. Our results indicate that the population of E/S0 galaxies is already in place at $z \sim 1$, in agreement with e.g. Lilly et al. (1995), Conselice et al. (2005), Zucca et al. (2006). As the field used in this paper is 160 arcmin^2 and includes large structures (Adami et al. 2005), cosmic variance could possibly play a role and affect our results. To investigate this point, we compare the global LF measured on the CDFS field with the LF in the VVDS-0226-04 field (Ilbert et al. 2005) which covers an area 10 times larger. Correcting the LF normalizations in the CDFS field to match the normalization of the global LF in the VVDS-0226-04 field, we find that the evolution, although less pronounced, still shows an increase of the red bulge-dominated density with the age of the Universe. The effect of the density-environment relation (e.g. Dressler et al. 1997) on

the observed evolution is difficult to assess. One approach to address this uncertainty is to compute the combined LF per morphological type and environment.

We also observe a very strong evolution of the blue bulge-dominated population corresponding to a brightening of 0.7 mag (or an increase in density by a factor 2.4) between $z \sim 0.6$ and $z \sim 1$. The nature of this population remains unclear. Mergers expected in the hierarchical scenario could create a burst of star formation explaining the blue color of these galaxies. We have observed some signs of disruption for a significant fraction of these galaxies. These galaxies could be also a dwarf population undergoing a strong burst of star formation in the galaxy core, which could be interpreted as a bulge component (Im et al. 2001). The smaller size of this blue population in comparison to the red one as well as the faint absolute magnitude distribution of this population seem to favor this hypothesis. Considering that the evolution of the blue bulge-dominated population produces a fading in luminosity, we can relate this evolution to the strong decrease of the star formation rate observed from $z \sim 1$. This blue population could be the progenitor of the local population of dwarf spheroidal galaxies undergoing strong star formation at $z \sim 1$. Another possibility to investigate is the presence of an AGN in the galaxy nucleus as shown by Menanteau et al. (2005) which could be strongly related to the star formation activity.

An increase in survey areas is clearly necessary to limit the cosmic variance effects on computing the LFs of morphologically selected populations, as is on-going with next generation surveys (e.g. COSMOS). The development of quantitative methods to better isolate morphological galaxy classes, in particular merger and irregular galaxies, and the combination of morphological and spectral classifications, will also be necessary for further progress.

Acknowledgements. This research has been developed within the framework of the VVDS consortium.
This work has been partially supported by the CNRS-INSU and its Programme National de Cosmologie (France), and by Italian Ministry (MIUR) grants COFIN2000 (MM02037133) and COFIN2003 (No. 2003020150).
The VLT-VIMOS observations have been carried out on guaranteed time (GTO) allocated by the European Southern Observatory (ESO) to the VIRMOS consortium, under a contractual agreement between the Centre National de la Recherche Scientifique of France, heading a consortium of French and Italian institutes, and ESO, to design, manufacture and test the VIMOS instrument.

References

Abraham, R. G., van den Bergh, S., Glazebrook, K., et al. 1996, ApJS, 107, 1
Adami, C., Mazure, A., Ilbert, O., et al. 2005, A&A, 443, 805
Arnouts, S., Vandame, B., Benoist, C., et al. 2001, A&A, 379, 740
Arnouts, S., Moscardini, L., Vanzella, E., et al. 2002, MNRAS, 329, 355
Bell, E. F., Papovich, C., Wolf, C., et al. 2005, ApJ, 625, 23
Brinchmann, J., Abraham, R., Schade, D., et al. 1998, ApJ, 499, 112
Bruzual, G., & Charlot, S. 2003, MNRAS, 344, 1000
Burgarella, D., Buat, V., Donas, J., Milliard, B., & Chapelon, S. 2001, A&A, 369, 421
Cassata, P., Cimatti, A., Franceschini, A., et al. 2005, MNRAS, 357, 903
Coleman, G. D., Wu, C.-C., & Weedman, D. W. 1980, ApJS, 43, 393
Conselice, C. J., Bershady, M. A., & Jangren, A. 2000, ApJ, 529, 886
Conselice, C. J., Blackburne, J. A., & Papovich, C. 2005, ApJ, 620, 564
Cross, N. J. G., Bouwens, R. J., Benítez, N., et al. 2004, AJ, 128, 1990
de Lapparent, V., Galaz, G., Bardelli, S., & Arnouts, S. 2003, A&A, 404, 831
Dressler, A., Oemler, A., Couch, W. J., et al. 1997, ApJ, 490, 577
Ferreras, I., Lisker, T., Carollo, C. M., Lilly, S. J., & Mobasher, B. 2005, ApJ, 635, 243
Giavalisco, M., Ferguson, H. C., Koekemoer, A., et al. 2004, ApJ, 600, L93
Ilbert, O., Tresse, L., Arnouts, S., et al. 2004, MNRAS, 351, 541
Ilbert, O., Tresse, L., Zucca, E., et al. 2005, A&A, 439, 863
Ilbert, O., Arnouts, S., McCracken, H. J., et al. 2006, A&A, submitted [arXiv:astro-ph/0603217]
Im, M., Simard, L., Faber, S. M., et al. 2002, ApJ, 571, 136
Im, M., Faber, S. M., Gebhardt, K., et al. 2001, AJ, 122, 750
Kuchinski, L. E., Madore, B. F., Freedman, W. L., & Trewhella, M. 2000, ApJS, 131, 441
Lauger, S., Burgarella, D., & Buat, V. 2005, A&A, 434, 77
Lauger, S., Ilbert, O., Burgarella, D., et al. 2006, A&A, submitted
Le Fèvre, O., Vettolani, G., Paltani, S., et al. 2004, A&A, 428, 1043
Le Fèvre, O., Vettolani, G., Garilli, B., et al. 2005, A&A, 439, 845
Lilly, S. J., Tresse, L., Hammer, F., Crampton, D., & Le Fèvre, O. 1995, ApJ, 455, 108
Madgwick, D. S., Lahav, O., Baldry, I. K., et al. 2002, MNRAS, 333, 133
Marinoni, C., Monaco, P., Giuricin, G., & Costantini, B. 1999, ApJ, 521, 50
Menanteau, F., Ford, H. C., Illingworth, G. D., et al. 2004, ApJ, 612, 202
Menanteau, F., Martel, A. R., Tozzi, P., et al. 2005, ApJ, 620, 697
Menanteau, F., Ford, H. C., Motta, V., et al. 2006, AJ, 131, 208
Nakamura, O., Fukugita, M., Yasuda, N., et al. 2003, ApJ, 125, 1682
Wolf, C., Meisenheimer, K., Rix, H.-W., et al. 2003, A&A, 401, 73
Wolf, C., Meisenheimer, K., Kleinheinrich, M., et al. 2004, A&A, 421, 913
Wolf, C., Bell, E. F., McIntosh, D. H., et al. 2005, AJ, 630, 771
Zucca, E., Ilbert, O., Tresse, L., et al. 2006, A&A, in press [arXiv:astro-ph/0506393]